

driven by the type of particle in which the Higgs bosons decays, and are somewhat softer.

C. Results on Φ^{SUSY}

The composition of the information on the neutralino annihilation cross section and branching ratios with the informations coming from the differential spectra of photons from the annihilation of neutralinos in pure final states provides the prediction of what we have called the supersymmetric factor Φ^{SUSY} in the γ -ray flux computation. Figure 8 shows Φ^{SUSY} defined as the integral of the gamma-ray flux of Eq. (2) above a set of sample threshold energies: 1, 10, 50, and 100 GeV. When the threshold energy is small, Φ^{SUSY} is roughly inversely proportional to the neutralino mass. Since the neutralinos annihilate almost at rest, when the threshold energy increases Φ^{SUSY} significantly drops because the highest available photon energy is $E \sim m_\chi$ for any given neutralino mass. The highest value for Φ^{SUSY} is of the order of $10^{-8} \text{ cm}^4 \text{ kpc}^{-1} \text{ s}^{-1} \text{ GeV}^{-2} \text{ sr}^{-1}$ when the threshold energy is 1 GeV. At masses larger than about 500 GeV for any given threshold energy the values of Φ^{SUSY} all lie inside a band which spans no more than 1 order of magnitude. This makes the predictions on the gamma-ray fluxes for large neutralino masses quite predictive: the possible variation due to the different supersymmetric models is confined to a relatively restricted range, much smaller than for the case of lighter neutralinos.

The information on the factor Φ^{SUSY} is detailed in Tables VII, VIII, and IX where we give the number of

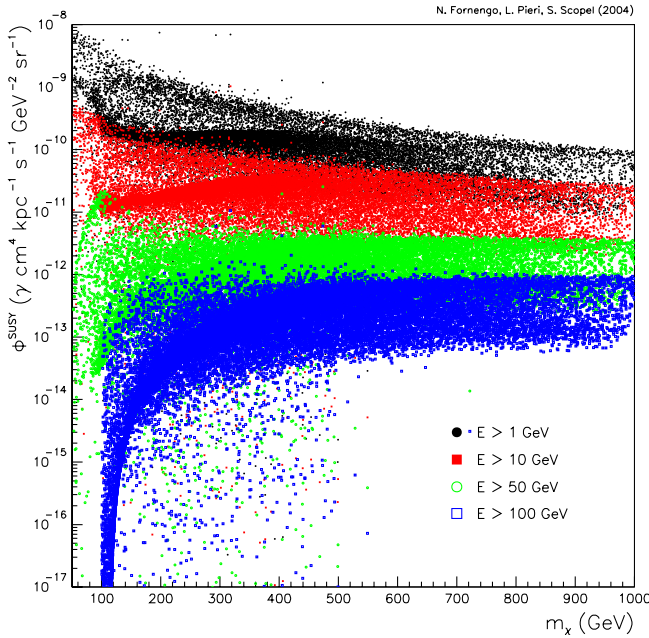


FIG. 8 (color online). The supersymmetric factor Φ^{SUSY} as a function of the neutralino mass. Different colors show different threshold energies above which the energy spectra have been integrated.

TABLE VII. Integrated number of photons above a given energy E from the annihilation of neutralinos with masses 500 GeV, 800 GeV, and 1 TeV, for different channels of annihilation.

	$m_\chi = 500 \text{ GeV}$	$m_\chi = 800 \text{ GeV}$	$m_\chi = 1 \text{ TeV}$
$\chi\chi \rightarrow u\bar{u} (d\bar{d})$			
$N_\gamma(>10 \text{ GeV})$	6.65	9.79	11.63
$N_\gamma(>50 \text{ GeV})$	0.91	1.78	2.37
$N_\gamma(>100 \text{ GeV})$	0.23	0.59	0.87
$N_\gamma(>500 \text{ GeV})$	0.00	1.9×10^{-3}	8.4×10^{-3}
$\chi\chi \rightarrow s\bar{s}$			
$N_\gamma(>10 \text{ GeV})$	6.61	9.83	11.71
$N_\gamma(>50 \text{ GeV})$	0.76	1.62	2.21
$N_\gamma(>100 \text{ GeV})$	0.15	0.46	0.73
$N_\gamma(>500 \text{ GeV})$	0.00	2.1×10^{-4}	1.7×10^{-3}
$\chi\chi \rightarrow c\bar{c}$			
$N_\gamma(>10 \text{ GeV})$	7.10	10.61	12.71
$N_\gamma(>50 \text{ GeV})$	0.69	1.60	2.19
$N_\gamma(>100 \text{ GeV})$	0.11	0.41	0.66
$N_\gamma(>500 \text{ GeV})$	0.00	8.7×10^{-5}	8.4×10^{-4}
$\chi\chi \rightarrow t\bar{t}$			
$N_\gamma(>10 \text{ GeV})$	5.03	8.65	10.81
$N_\gamma(>50 \text{ GeV})$	0.29	0.84	1.29
$N_\gamma(>100 \text{ GeV})$	0.04	0.17	0.30
$N_\gamma(>500 \text{ GeV})$	0.00	1.7×10^{-4}	8.1×10^{-4}
$\chi\chi \rightarrow b\bar{b}$			
$N_\gamma(>10 \text{ GeV})$	7.02	11.02	13.31
$N_\gamma(>50 \text{ GeV})$	0.49	1.26	1.83
$N_\gamma(>100 \text{ GeV})$	0.07	0.28	0.47
$N_\gamma(>500 \text{ GeV})$	0.00	5.8×10^{-5}	6.3×10^{-4}
$\chi\chi \rightarrow \text{gluons}$			
$N_\gamma(>10 \text{ GeV})$	6.42	10.69	13.18
$N_\gamma(>50 \text{ GeV})$	0.34	0.95	1.47
$N_\gamma(>100 \text{ GeV})$	0.04	0.17	0.32
$N_\gamma(>500 \text{ GeV})$	0.00	5.7×10^{-5}	4.3×10^{-4}

photons produced in each pure final state for different threshold energies. This information may be used to make predictions for the gamma-ray fluxes also for DM candidates other than the neutralino.

The results of this section and of Sec. III will be used in the next sections to predict the photon fluxes from the galactic center and from our representative external galaxies.

V. PREDICTION AND DETECTABILITY OF PHOTON FLUXES

In this section we will show the results on the prediction of photon fluxes from neutralino annihilation in our Galaxy and in some selected external galaxies. We will therefore study the detectability of such signals with ground-based Čerenkov telescopes and next generation satellite-borne experiments.

TABLE VIII. Integrated number of photons above a given energy E from the annihilation of neutralinos with masses 500 GeV, 800 GeV, and 1 TeV, for different channels of annihilation.

	$m_\chi = 500$ GeV	$m_\chi = 800$ GeV	$m_\chi = 1$ TeV
$N_\gamma(>500$ GeV)	0.00	5.8×10^{-5}	6.3×10^{-4}
$\chi\chi \rightarrow \tau^+\tau^-$			
$N_\gamma(>10$ GeV)	2.19	2.38	2.46
$N_\gamma(>50$ GeV)	1.16	1.55	1.72
$N_\gamma(>100$ GeV)	0.58	0.98	1.28
$N_\gamma(>500$ GeV)	0.00	3.3×10^{-2}	8.2×10^{-2}
$\chi\chi \rightarrow W^+W^-$			
$N_\gamma(>10$ GeV)	4.76	7.15	8.45
$N_\gamma(>50$ GeV)	0.52	1.14	1.57
$N_\gamma(>100$ GeV)	0.11	0.34	0.52
$N_\gamma(>500$ GeV)	0.00	1.3×10^{-3}	4.4×10^{-3}
$\chi\chi \rightarrow ZZ$			
$N_\gamma(>10$ GeV)	4.96	7.67	9.19
$N_\gamma(>50$ GeV)	0.48	1.12	1.57
$N_\gamma(>100$ GeV)	0.09	0.30	0.49
$N_\gamma(>500$ GeV)	0.00	0.9×10^{-3}	3.1×10^{-3}

A. Predicted photon fluxes from neutralino annihilation

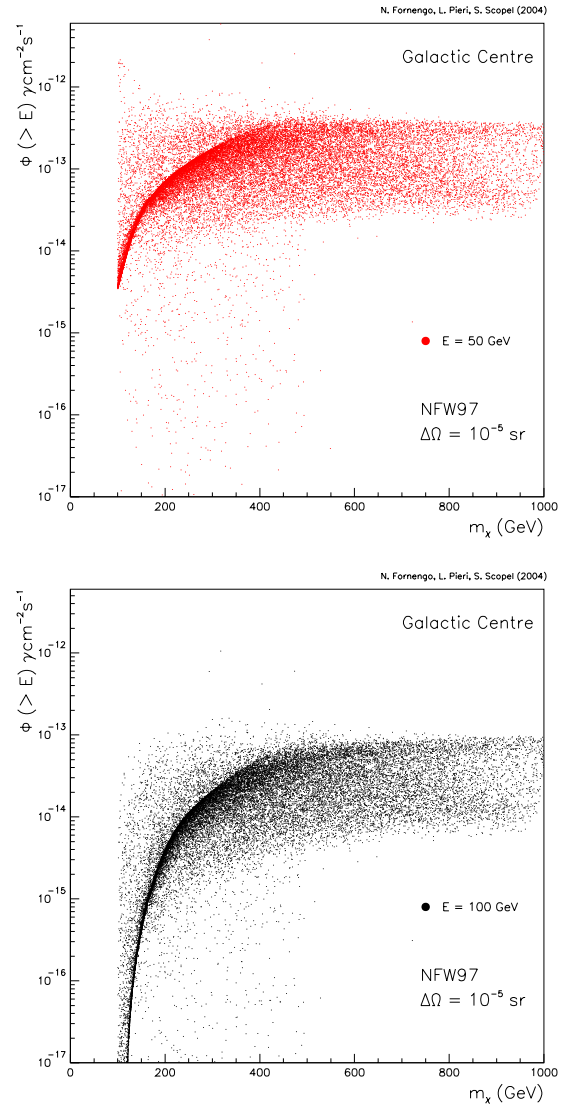
In the previous sections we have computed the cosmological factor Φ^{cosmo} (see Fig. 2) and the supersymmetric factor Φ^{SUSY} (see Fig. 8). We are now ready to predict the gamma-ray fluxes from neutralino annihilation in the

 TABLE IX. Integrated number of photons above a given energy E from the annihilation of 1 TeV neutralino into a sample state of Higgs bosons, with subsequent decay into b quarks or tau leptons. A mass of 120 GeV has been assumed for the light Higgs, while a mass of 500 GeV has been taken for the charged, heavy and pseudoscalar Higgs's.

	$\chi\chi \rightarrow \text{Higgs}$	
	$hh \rightarrow b\bar{b}$	$hh \rightarrow \tau^+\tau^-$
$N_\gamma(>10$ GeV)	13.95	3.89
$N_\gamma(>50$ GeV)	1.56	1.97
$N_\gamma(>100$ GeV)	0.34	1.07
$N_\gamma(>500$ GeV)	1.8×10^{-4}	0.02
	$AA(HH) \rightarrow b\bar{b}$	$AA(HH) \rightarrow \tau^+\tau^-$
$N_\gamma(>10$ GeV)	13.32	4.00
$N_\gamma(>50$ GeV)	1.37	2.01
$N_\gamma(>100$ GeV)	0.27	1.09
$N_\gamma(>500$ GeV)	6.8×10^{-5}	0.02
	$H^+H^- \rightarrow b\bar{b}$	$H^+H^- \rightarrow \tau^+\tau^-$
$N_\gamma(>10$ GeV)	11.41	2.00
$N_\gamma(>50$ GeV)	1.00	1.00
$N_\gamma(>100$ GeV)	0.17	0.54
$N_\gamma(>500$ GeV)	7.4×10^{-5}	0.01

effective MSSM. Results are reported in Figs. 9 and 10, where we show the expected fluxes of γ rays with energies above 50 GeV and 100 GeV from the galactic center and M31 and for a detector aperture of $\Delta\Omega = 10^{-5}$ sr. Figure 9 refers to the galactic center for a Milky Way with an NFW97 density profile, while Fig. 10 is calculated for M31 with an M99 density profile. The spread of points is given by the different SUSY parameters corresponding to each point.

In the case of the flux from the galactic center with an NFW97 profile and a typical threshold energy of 50 GeV, we predict a maximal gamma-ray flux of the order of 10^{-12} $\text{cm}^{-2}\text{s}^{-1}$ for neutralinos lighter than 200 GeV, while heavier neutralinos can provide a maximal flux of


 FIG. 9 (color online). Integrated gamma-ray fluxes from neutralino annihilation at the galactic center, for an NFW97 density profile and inside a solid angle $\Delta\Omega = 10^{-5}$ sr. Two representative threshold energies have been assumed: 50 GeV (upper panel) and 100 GeV (lower panel).